Letter

Nonlinear Photon Pair Generation in a Highly Dispersive Medium

David J. Starling,[1,*] Jacob Poirier,[2] Michael Fanto,[3,4] Jeffrey A. Steidle,[4] Christopher C. Tison,[3] Gregory A. Howland,[2,4] and Stefan F. Preble[4]

[1] *Division of Science, Pennsylvania State University, Hazleton, Pennsylvania 18202, USA*
[2] *School of Physics and Astronomy, Rochester Institute of Technology, Rochester, New York 14623, USA*
[3] *Air Force Research Laboratory, Rome, New York 13441, USA*
[4] *Microsystems Engineering, Rochester Institute of Technology, Rochester, New York 14623, USA*

(Received 3 January 2020; revised manuscript received 11 February 2020; accepted 6 April 2020; published 29 April 2020)

Photon pair generation in silicon photonic integrated circuits relies on four-wave mixing via the third-order nonlinearity. Due to phase matching requirements and group velocity dispersion, this method has typically required TE-polarized light. Here, we demonstrate TM-polarized photon pair production in linearly uncoupled silicon resonators with more than an order of magnitude greater dispersion than in previous work. We achieve measured rates above 2.8 kHz and a conditional self-correlation of $g^{(2)}(0) = 0.044 \pm 0.004$. This method enables phase matching in dispersive media and paves the way for entanglement generation in silicon photonic devices.

DOI: 10.1103/PhysRevApplied.13.041005

Photonic integrated circuits (PICs) provide a miniature, stable, and scalable platform for developing future light-based quantum technologies, including sensors, secure communications, and information processors [1]. These systems require the on-chip generation of high-quality single photons or correlated photon pairs [2]. The required on-chip photon source is bright, efficient, and scalable and produces indistinguishable or heralded photons.

There is strong motivation to realize these quantum PICs in silicon at telecommunications wavelengths. Such developments can leverage both the existing CMOS electronics fabrication and manufacturing processes as well as the widespread telecommunications fiber-optic infrastructure. Consequently, significant effort has been devoted towards silicon-photonic photon source development [3,4]. Since silicon lacks a second-order optical nonlinearity, spontaneous four-wave mixing (SFWM)—a weaker third-order effect—is utilized. In order to increase source brightness, many employ resonant structures such as microring [5] or microdisk [6] resonators to increase the effective interaction length. While these resonant sources enhance the source brightness, precise control is required to generate and extract photon pairs from the resonator [7]. Methods to reduce parasitic processes [8] and enhance extraction efficiency [9] are active areas of research.

Furthermore, the large polarization mode dispersion in silicon waveguides has limited resonant photon pair generation to just the TE polarization [10]. Zeng and Popović [11] and Zeng *et al.* [12] demonstrated dispersion engineering via the use of three coupled resonators that were independently tunable. Recently, Menotti *et al.* proposed a FWM scheme in a pair of resonators that are nonlinearly coupled but linearly uncoupled [13]. In this system, only one set of correlated energy modes are enhanced and able to transfer between the two resonators. They went on to experimentally demonstrate a classical, seeded device using low-dispersion TE-polarized light with nonlinear mixing between frequency modes [14].

In this letter, we experimentally demonstrate a similar dual-resonator correlated photon source for highly dispersive TM-polarized light. We produce high-quality, heralded single photons at detection rates up to 2.8 kHz with $g^{(2)}(0) = 0.044 \pm 0.004$ near 1550 nm. Our results show that resonant enhancement of photon generation in highly dispersive media is possible, paving the way for a variety of applications. These include telecommunication-to-visible frequency conversion [15] and the generation of hyper-entangled photons, with entanglement between polarization, path, energy, and time [16].

We begin by considering two racetrack-style resonators that are critically coupled to separate waveguides, as shown in Fig. 1(a). Each resonator can be independently tuned via resistive heating with voltages applied at V_1 and V_2. The two resonators interact via a directional coupler (DC) that is designed to ensure input light remains within resonator one. In this way, the two resonators are linearly uncoupled. Pump light (green in the figure) is directed in through the input port, on resonance with resonator one. Due to the third-order nonlinearity in silicon, signal and

*starling@psu.edu

idler photons in a wide range of wavelengths can be generated via SFWM in the first resonator. However, in the DC, signal and idler photons that are resonant with resonator two are interferometrically enhanced, and couple into resonator two (blue and red in the figure). Therefore, the two resonators are nonlinearly coupled. We note though that SFWM will only be enhanced when the resonances are equally spaced about the pump wavelength, a strict requirement for energy conservation. However, since the two resonators can be independently controlled, it is possible to realize efficient photon pair generation (alignment of the resonances) even in the case where the individual resonators are highly dispersive [13,14].

Here we focus on nondegenerate SFWM photon pair generation using TM-polarized light, which has a large group velocity dispersion (order of magnitude larger than that of TE). We also obtain the advantages expected by the authors of Ref. [13]: namely, enhancement of the SFWM process, reduction of parasitic processes, compensation of self-phase-modulation, and less restrictive requirements on phase matching.

We now turn to the experimental details. Light from a tunable, narrow-band laser near 1550 nm is directed through a variable optical attenuator and polarization controller and then into the PIC (see Fig. 1). The PIC is fabricated through the Applied Nanotools Inc. NanoSOI prototyping service and is a silicon-on-insulator device with 500×220 nm^2 waveguides defined through electron-beam lithography, trilayer metalization, and oxide deposition. The 600-nm gap between the pump waveguide (input and through) and resonator one is the same as the gap between the output waveguide (add and drop) and resonator two. The DC, where the nonlinear interaction is enhanced, has a gap of 250 nm and is $L = 18$ μm long (designed to have zero linear coupling between the resonators). Resonators one and two have a round-trip length of $\mathcal{L}_1 = 138$ μm and $\mathcal{L}_2 = 130$ μm, respectively. The PIC is secured with a temperature-controlled vacuum mount held at 27.2 °C.

A single-mode fiber (SMF-28) is fusion-spliced to an ultrahigh-numerical-aperture fiber to improve fiber-to-PIC coupling [17], with a fiber-to-chip loss of approximately 2.7 dB per facet. The through and drop ports are coupled and directed either to a high-speed power meter or through a coarse wavelength division multiplexer, polarization controllers, low-loss tunable grating filters (F1 and F2), and finally superconducting nanowire single-photon detectors (SNSPDs) operating below 0.80 K. The total measured losses from the chip to the SNSPDs are approximately 9.0 and 5.7 dB for the signal and idler photons, respectively. We perform correlation measurements using a PicoHarp 300 (for standard coincidence detection) and a Swabian Time Tagger 20 (for conditioned $g^{(2)}$ measurements).

First, to characterize the resonances, we scan the input pump wavelength and measure the transmission as shown in Fig. 1(b). Resonators one and two have loaded quality factors of approximately 4.1×10^5 and 3.7×10^5, respectively. Note that these scans are not corrected for losses, but instead measured as the total round-trip loss from laser to detector. Measuring the power from the input port to the through port results in the green curve (the pump channel), while measuring from the add port to the drop port results in the blue and red curves (the signal and idler channels). We see that the two resonators are linearly uncoupled; additionally, each set of resonances have approximately -15 to -17 dB of coupling. When voltage V_2 is applied to the heater of the second resonator, the resonances shift via resistive heating with minimal shift (cross-talk) on resonator one. By centering (in frequency) the resonances of resonator two around a single resonance of resonator one, we ensure energy conservation in the SFWM process.

In what follows, we focus on light generation between signal-idler fields that are three free spectral ranges (FSR, $\Delta\lambda_{\mathrm{FSR}}$) apart to demonstrate phase matching with large dispersion. Additionally, we note here that there is no evidence of TE-polarized light found in the drop port (in neither the resonance scans nor the single-photon experiments detailed below).

Using the resonance information from Fig. 1(b), we calculate the group index dispersion without the need for Fourier analysis [18]. The results are shown in Fig. 1(c) using the relation $n_g = \lambda^2/\Delta\lambda_{\mathrm{FSR}}L$. In this calculation, we have averaged the results for the two resonators due to a slight discrepancy between the two curves. This discrepancy is likely due to the varied effect of the DC on each resonator. We apply a moving average since the frequency of the peaks for each resonator is unique; however, the slope of the curve should not be affected. We see a large change in group index with a dispersion parameter of $D = -32\,000$ ps/nm-km (group velocity dispersion of -40.4 ps^2/m), confirming that we analyze and measure TM-polarized light; this result is consistent with that of other work that required Fourier analysis [18].

Utilizing the tunability of the resonators, we generate photon pairs via the SFWM process. We measure time correlations with a bin width of 32 ps and choose a coincidence window of 448 ps, as shown in the top right of Fig. 1. The curve shows a Gaussian fit with a FWHM of 227 ps. We optimize the photon pair count rate by varying the pump wavelength and heater temperature to account for phase matching and self-phase-modulation. Coincidences are calculated by summing coincidence counts within the coincidence window and subtracting accidental coincidences from an equivalent, far away integration window. The coincidence-to-accidental ratio (CAR) is found by dividing the same two numbers. We obtain a maximum measured count rate of 2855 Hz with a CAR of 237,

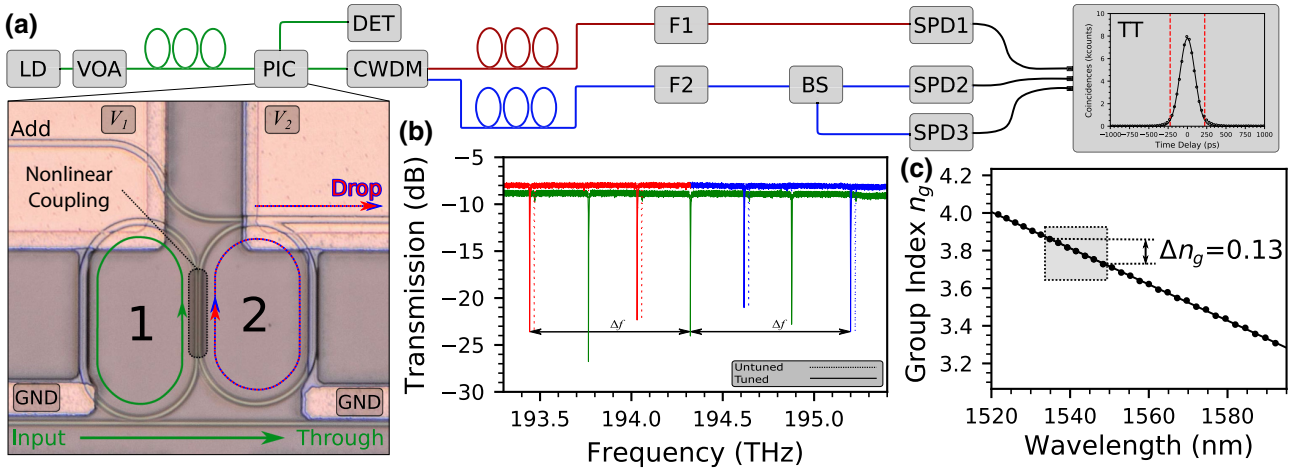

FIG. 1. Experimental setup. (a) Light from a laser (LD) passes through a variable optical attenuator (VOA) and polarization controller and then enters the PIC. Light is collected from the PIC and sent either to a detector (DET) or through a coarse wavelength division multiplexer (CWDM) to separate signal and idler photons. Each path then passes through polarization controllers and filters (F1 and F2). Signal photons are separated at a 50:50 beam splitter (BS) and then photons are detected via superconducing nanowire single-photon detectors (SPDs) and correlated with a time tagger (TT). PIC showing the input pump field (green) and the signal and idler photons (blue and red) created in the DC and extracted through the drop port. Voltages V_1 and V_2 are applied to tune the first and second resonators, respectively. (b) The transmission through the PIC from the input port to the through port (green) and the add port to the drop port [blue (signal side) and red (idler side)] is shown. The green resonances correspond to resonator one and the blue and red resonances correspond to resonator two. The dashed curve shows the untuned resonances of resonator two, resulting in poor phase matching. The solid curve shows a symmetric resonance structure, allowing for energy conservation and efficient SFWM. The symmetric solid curve shows the frequency shift Δf between the pump and the signal and idler. (c) The averaged measured group index as determined by the free spectral range from (b). The region where the experiments are conducted is highlighted, showing the large change in group index.

similar to other nanophotonic devices [19,20]. These values are obtained with approximately 2.1 mW in the input waveguide. However, we find that the value of CAR is not a simple function of input power, perhaps due to the bistability of the input resonator, compensation of self-phase-modulation, or interferometric enhancement from the second resonator. We calculate our Klyshko efficiency via the standard method ($\eta_K = N_{\rm si}/N_s$) [6] to reach up to 7% when the heater is optimized, similar to other methods [15].

The pair generation rate in this system, compared to a standard microring resonator of length $\mathcal{L}_1$, should be reduced by a factor of $L/4\mathcal{L}_1 = 3.26\%$. This is due to the shorter effective interaction length L and opposite phase oscillations of the pump and signal fields [13]. Despite this, we estimate a maximum pair generation rate of approximately 1.3×10^5 Hz by accounting for losses between the PIC and the SNSPDs. This implies that a single resonator of the same length $\mathcal{L}_1$ would result in a pair generation rate of 4.0×10^6, in rough agreement with previous results [21]. Normalized by the FWHM of the loaded resonator and input waveguide power squared, we achieve a spectral brightness of 5.5×10^4 pairs $\rm s^{-1}\,GHz^{-1}\,mW^{-2}$.

To confirm that the dominant pair generation processes rely on the nonlinear coupling of the two resonators, we vary the heater current of resonator two in order to shift its resonances. We measure coincidences for 3 min at each setting and the results are shown in Fig. 2 with accidental coincidences subtracted. The horizontal axis is calibrated by measuring the shift in resonances shown in Fig. 1(b) as a function of current. The full width at half maximum of a Lorentzian least-squares fit is found to be 2.98 GHz, confirming that efficient photon pair generation requires the resonances to be precisely aligned for energy conservation.

Since the SFWM process is nonlinear, we vary the input power to demonstrate the expected quadratic dependence as shown in Fig. 3. For each setting, the input power is set (with a maximum power of approximately 0.5 mW) and the pump frequency and resonances of resonator two are scanned to optimize coincidence counts. Then, a 20-s integration at the optimum scanned setting is acquired and accidental coincidences are subtracted.

Lastly, to analyze the quantum properties of the photon pairs, we perform a conditional second-order self-correlation measurement ($g^{(2)}$) as shown in Fig. 4 [22]. We accomplish this by splitting the signal photons with a 50:50 fiber-optic coupler into channels 2 and 3 and conduct a standard second-order coherence measurement *conditioned* on a detection in channel 1 [4,23,24]:

$$g^{(2)}(t_3) = \frac{N_{123}(t_3)N_1}{N_{12}N_{13}(t_3)}. \quad (1)$$

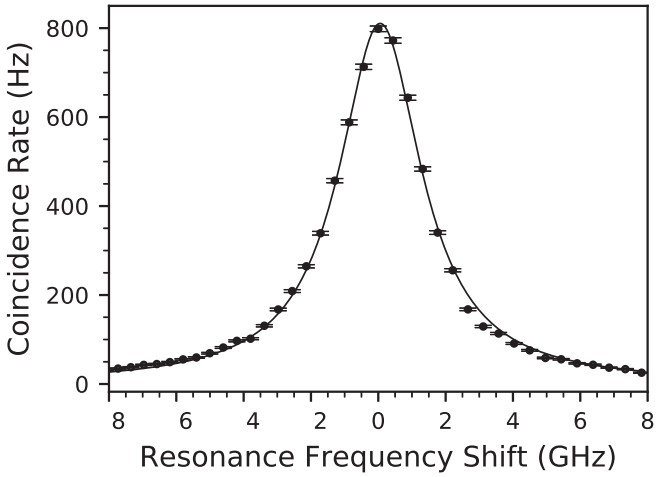

FIG. 2. The locations of the resonances for resonator two are scanned via resistive heating. We include a Lorentzian least-squares fit with a FWHM of 2.98 GHz. Each data point is collected with 3.0 min of integration.

We report the results by varying the time delay between channels 2 and 3, using detection events in channel 1 as a gate to condition, and measuring triple coincidences as shown in Fig. 4(a) [25,26]. In Fig. 4(b), we hold $t_1 = t_2 = 0$ fixed and vary t_3; the results for varying t_2 instead are similar. With approximately 2.1 mW of power in the input waveguide yielding 242-Hz coincidences, we measure $g^{(2)}(0) = 0.044 \pm 0.004$, over 200 standard deviations below the classical threshold.

In conclusion, despite large group velocity dispersion, we demonstrate phase matching in the SFWM process, made possible by the relatively short interaction length

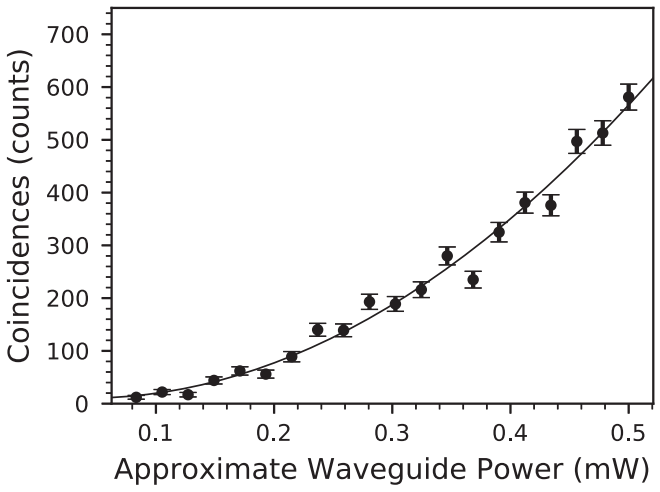

FIG. 3. The input pump power is varied and coincidences are measured, exhibiting the quadratic behavior of the device. Error bars enclose one standard deviation. Input waveguide power is approximated based upon loss measurements. Values above 0.5 mW begin to saturate the quadratic pair generation rate.

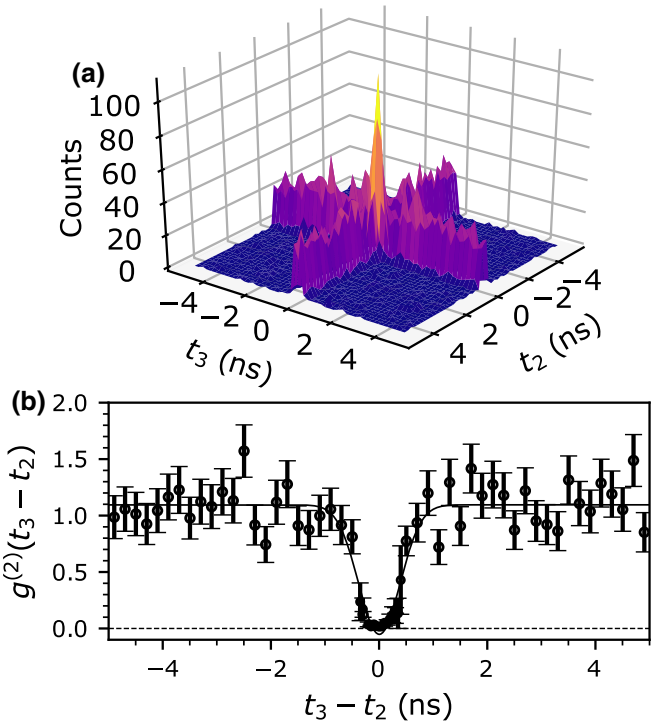

FIG. 4. (a) A histogram of the number of triple coincidences between channels 1, 2, and 3, with $t_1 = 0$. (b) The value of $g^{(2)}$ as a function of the time delay between channels 2 and 3, where $t_1 = t_2 = 0$. These data include two sets of 10 h of integration (with bin sizes of 200 and 50 ps) and an average coincidence rate of 437 Hz. We show only the data for the smaller bin size near $t_3 - t_2 = 0$ where triple coincidences are more common and error bars are small. A Gaussian fit to both sets of data combined gives a FWHM of 904 ps.

in the nonlinear coupling region and the interferometric enhancement of the second resonator. The process is sensitive to the tuning of the "readout" resonator and coincidences show a quadratic dependence on input pump power. We obtain a maximum measured count rate of 2855 Hz with a CAR of 237 using 2.1 mW of pump power in the waveguide. We obtain these results using only a single pump-rejection filter on each output channel. Furthermore, we do not employ a polarization-maintaining fiber, or filter the pump to limit amplified spontaneous emission or Raman scattering.

We have also shown single-photon quantum behavior in a silicon resonator using highly dispersive TM-polarized light with a group velocity dispersion more than one order of magnitude larger than that of previous systems (-40.4 ps^2/m vs $+1.33$ ps^2/m) [21]. We note here that the phase mismatch Δ is linear in terms of the dispersion parameter D and quadratic in the detuning Ω: $\Delta \approx -D\lambda^2\Omega^2/2\pi c$ [27]. Given that D is a factor of 30 larger for TM than TE, we predict that phase matching is possible over an even larger frequency range ($\sqrt{30} \approx 5.5$) utilizing TE-polarized light

with this method. These results allow for the creation of hyper-entangled photons using polarization, path, time, and energy in a silicon platform. Additionally, this process may be applicable to telecommunication-to-visible spectral transduction of entangled photons given the flexibility in phase matching. Lastly, we believe this work has implications for phase matching in nonlinear processes more generally, and may be of interest to the nanophotonic spontaneous parametric down-conversion community [28].

ACKNOWLEDGMENTS

This work was supported by the Pennsylvania State University and the Air Force Research Laboratory (FA8750-16-2-0140). Any opinions, findings, and conclusions or recommendations expressed in this material are those of the author(s) and do not necessarily reflect the views of the AFRL.

[1] Jianwei Wang, Fabio Sciarrino, Anthony Laing, and Mark G. Thompson, Integrated photonic quantum technologies, Nat. Photonics, 1 (2019).

[2] Alexander W. Bruch, Xianwen Liu, Xiang Guo, Joshua B. Surya, Zheng Gong, Liang Zhang, Junxi Wang, Jianchang Yan, and Hong X. Tang, 17000%/w second-harmonic conversion efficiency in single-crystalline aluminum nitride microresonators, Appl. Phys. Lett. **113**, 131102 (2018).

[3] J. W. Silverstone, D. Bonneau, J. L. O'Brien, and M. G. Thompson, Silicon quantum photonics, IEEE J. Sel. Top. Quantum Electron. **22**, 390 (2016).

[4] Chaoxuan Ma, Xiaoxi Wang, Vikas Anant, Andrew D. Beyer, Matthew D. Shaw, and Shayan Mookherjea, Silicon photonic entangled photon-pair and heralded single photon generation with car $> 12,000$ and $g(2)(0) < 0.006$, Opt. Express **25**, 32995 (2017).

[5] Farid Samara, Anthony Martin, Claire Autebert, Maxim Karpov, Tobias J. Kippenberg, Hugo Zbinden, and Rob Thew, High-rate photon pairs and sequential time-bin entanglement with Si_3N_4 microring resonators, Opt. Express **27**, 19309 (2019).

[6] Xiyuan Lu, Steven Rogers, Thomas Gerrits, Wei C. Jiang, Sae Woo Nam, and Qiang Lin, Heralding single photons from a high-Q silicon microdisk, Optica **3**, 1331 (2016).

[7] C. C. Tison, J. A. Steidle, M. L. Fanto, Z. Wang, N. A. Mogent, A. Rizzo, S. F. Preble, and P. M. Alsing, Path to increasing the coincidence efficiency of integrated resonant photon sources, Opt. Express **25**, 33088 (2017).

[8] Mikkel Heuck, Jacob Gade Koefoed, Jesper Bjerge Christensen, Yunhong Ding, Lars Hagedorn Frandsen, Karsten Rottwitt, and Leif Katsuo Oxenløwe, Unidirectional frequency conversion in microring resonators for on-chip frequency-multiplexed single-photon sources, New J. Phys. **21**, 033037 (2019).

[9] Mikkel Heuck, Mihir Pant, and Dirk R. Englund, Temporally and spectrally multiplexed single photon source using quantum feedback control for scalable photonic quantum technologies, New J. Phys. **20**, 063046 (2018).

[10] K. Harada, H. Takesue, H. Fukuda, T. Tsuchizawa, T. Watanabe, K. Yamada, Y. Tokura, and S. Itabashi, Frequency and polarization characteristics of correlated photon-pair generation using a silicon wire waveguide, IEEE J. Sel. Top. Quantum Electron. **16**, 325 (2010).

[11] Xiaoge Zeng and Miloš A. Popović, Design of triply-resonant microphotonic parametric oscillators based on kerr nonlinearity, Opt. Express **22**, 15837 (2014).

[12] Xiaoge Zeng, Cale M. Gentry, and Miloš A. Popović, Four-wave mixing in silicon coupled-cavity resonators with port-selective, orthogonal supermode excitation, Opt. Lett. **40**, 2120 (2015).

[13] M. Menotti, B. Morrison, K. Tan, Z. Vernon, J. E. Sipe, and M. Liscidini, Nonlinear Coupling of Linearly Uncoupled Resonators, Phys. Rev. Lett. **122**, 013904 (2019).

[14] K. Tan, M. Menotti, Z. Vernon, J. E. Sipe, M. Liscidini, and B. Morrison, Stimulated four-wave mixing in linearly uncoupled resonators, Opt. Lett. **45**, 873 (2020).

[15] C. Söller, B. Brecht, P. J. Mosley, L. Y. Zang, A. Podlipensky, N. Y. Joly, P. St. J. Russell, and C. Silberhorn, Bridging visible and telecom wavelengths with a single-mode broadband photon pair source, Phys. Rev. A **81**, 031801(R) (2010).

[16] Julio T. Barreiro, Nathan K. Langford, Nicholas A. Peters, and Paul G. Kwiat, Generation of Hyperentangled Photon Pairs, Phys. Rev. Lett. **95**, 260501 (2005).

[17] Peichuan Yin, John R. Serafini, Zhan Su, Ren-Jye Shiue, Erman Timurdogan, Michael L. Fanto, and Stefan Preble, Low connector-to-connector loss through silicon photonic chips using ultra-low loss splicing of SMF-28 to high numerical aperture fibers, Opt. Express **27**, 24188 (2019).

[18] Daniel Pergande and Ralf B. Wehrspohn, Losses and group index dispersion in insulator-on-silicon-on-insulator ridge waveguides, Opt. Express **18**, 4590 (2010).

[19] Jiakun He, Bryn A. Bell, Alvaro Casas-Bedoya, Yanbing Zhang, Alex S. Clark, Chunle Xiong, and Benjamin J. Eggleton, Ultracompact quantum splitter of degenerate photon pairs, Optica **2**, 779 (2015).

[20] Pisek Kultavewuti, Eric Y. Zhu, Li Qian, Vincenzo Pusino, Marc Sorel, and J. Stewart Aitchison, Correlated photon pair generation in algaas nanowaveguides via spontaneous four-wave mixing, Opt. Express **24**, 3365 (2016).

[21] Marc Savanier, Ranjeet Kumar, and Shayan Mookherjea, Photon pair generation from compact silicon microring resonators using microwatt-level pump powers, Opt. Express **24**, 3313 (2016).

[22] Imad I. Faruque, Gary F. Sinclair, Damien Bonneau, Takafumi Ono, Christine Silberhorn, Mark G. Thompson, and John G. Rarity, Estimating the Indistinguishability of Heralded Single Photons Using Second-Order Correlation, Phys. Rev. Appl. **12**, 054029 (2019).

[23] M. Beck, Comparing measurements of g(2)(0) performed with different coincidence detection techniques, J. Opt. Soc. Am. B **24**, 2972 (2007).

[24] K. Laiho, A. Christ, K. N. Cassemiro, and C. Silberhorn, Testing spectral filters as gaussian quantum optical channels, Opt. Lett. **36**, 1476 (2011).

[25] M. Razavi, I. Söllner, E. Bocquillon, C. Couteau, R. Laflamme, and G. Weihs, Characterizing heralded

single-photon sources with imperfect measurement devices, J. Phys. B: At. Mol. Opt. Phys. **42**, 114013 (2009).

[26] Alessia Allevi, Stefano Olivares, and Maria Bondani, Measuring high-order photon-number correlations in experiments with multimode pulsed quantum states, Phys. Rev. A **85**, 063835 (2012).

[27] Govind P. Agrawal, *Fiber–Optic Communication Systems* (Wiley, New York, 2010), 4th ed.

[28] Xiang Guo, Chang-ling Zou, Carsten Schuck, Hojoong Jung, Risheng Cheng, and Hong X. Tang, Parametric down-conversion photon-pair source on a nanophotonic chip, Light Sci. Appl. **6**, e16249 (2017).